

## Particle motion in mixed flow dryers

Tamás Tolnai \*

*Rail Safe Kft., 5051 Zagyarékas, Csárda utca 31-43. Hungary.*

Global Journal of Engineering and Technology Advances, 2021, 09(03), 114–121

Publication history: Received on 17 November 2021; revised on 22 December 2021; accepted on 24 December 2021

Article DOI: <https://doi.org/10.30574/gjeta.2021.9.3.0171>

### Abstract

Differences in flow rates of this nature have a significant effect on the unevenness of the moisture content of the dried material, since the material which remains in the drying chamber for an unnecessarily long time is over-dried and the under-drying is a problem for the material remaining in the dryer for too short a time. In this article, I analyzed the effect of increasing particle-wall friction on the unevenness of the particle flow velocity field. The research has shown that dead zones are formed in the vicinity of the rough walls, which reduce the uniformity of the flow. The results show that the tribological properties of the inner wall surfaces of the dryers can have a very significant effect on the efficient operation of the dryers.

**Keywords:** Particle motion; Moisture content; Uniform flow; Uniform drying; Flow rate

### 1. Introduction

Drying of grain crops before storage is an essential task in agriculture. The cost of drying is very high, and its incorrect implementation endangers the quality of the grain to be stored. To avoid under- and over-drying, it is necessary to know as much as possible about the material flow processes that take place in the drying equipment. Accurate knowledge of grain motion is also an important part of this task. Mellmann et al. 2011 [1,2] created the basic equations of particle flow in dryers and evaluated and measured the residence time distribution.

#### 1.1. Discrete element method (DEM)

The discrete element method is an explicit dynamical modelling procedure that models the mechanical behaviour of particle assemblies at the level of interactions between individual particles. As a result, it is an extremely computationally intensive modelling method that requires significant IT resources. The discrete element method was developed by Cundall and Strack in 1979 [3] to study rock mechanical problems in the late 1970s. The increase in computational capacity since then has made it possible to further develop the method and make it suitable for solving practical problems as well.

Using discrete element model, the contact forces formed during the collision between the particles can be determined using the Hertz-Mindlin contact model. DEM models the coupling of the particles using springs and dampers for the calculations (Fig. 1).

\* Corresponding author: Tamás Tolnai  
Rail Safe Kft., 5051 Zagyarékas, Csárda utca 31-43. Hungary.

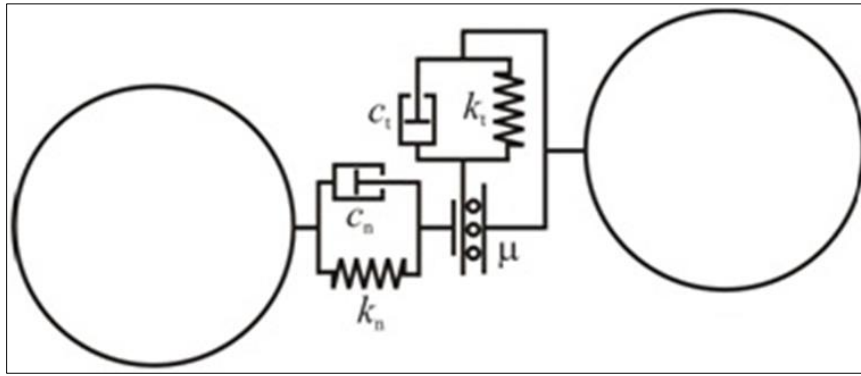


**Figure 1** Spring, damper model of particle contact

The normal force is calculated as:

$$F_n = \frac{4}{3} E_0 \delta^{\frac{3}{2}} \sqrt{R_0} - 2 \sqrt{\frac{5}{6} \frac{\ln C_r}{\sqrt{\ln^2 C_r + \pi^2}}} \sqrt{2 E_0^4 \sqrt{R_0} \delta} \sqrt{m_0} v_{nrel}$$

where:

$$\frac{1}{E_0} = \frac{1 - \nu_1^2}{2(1 + \nu_1)G_1} + \frac{1 - \nu_2^2}{2(1 + \nu_2)G_2}$$

is the reduced Young modulus of the two particles,  $\delta$  is the compression between the two particles,

$$R_0 = \frac{R_1 R_2}{R_1 + R_2}$$

is the reduced radius,

$$m_0 = \frac{m_1 m_2}{m_1 + m_2}$$

is the reduced mass,  $v_{nrel}$  is the normal component of the two particle's relative velocity.

The tangential force is:

$$F_t = -8G_0 \sqrt{R_0} \delta \delta_t - 2 \sqrt{\frac{5}{6} \frac{\ln C_r}{\sqrt{\ln^2 C_r + \pi^2}}} \sqrt{2G_0^4 \sqrt{R_0} \delta} \sqrt{m_0} v_{trel}$$

where:

$$\frac{1}{G_0} = \frac{2 - \nu_1}{G_1} + \frac{2 - \nu_2}{G_2}$$

is the reduced shear modulus,  $\delta_t$  is the tangential deformation  $v_{trel}$  is the tangential component of the two particle's relative velocity.

The maximum possible value of the tangential force is limited by Coulomb's law of friction:

$$F_t \leq \mu_s F_n$$

where  $\mu_s$  is the coefficient of static friction.

The torque of rolling friction:

$$M_r = \mu_r F_N R_i \omega_i$$

where  $R_i$  is the distance of the contact point from the centre of the  $i$ -th particle,  $\omega_i$  is the angular velocity of the particle. The torque of the tangential force:

$$M_t = F_t R_i$$

must also be considered.

During the simulation it has to be sure that the time scale is chosen correctly, this has a significant effect on the stability of the numerical model. In the calculations, I used 25% of the Rayleigh time scale

$$T = 0,25T_R = 0,25 \cdot (0,1631\nu + 0,8766)^{-1} \pi R \left( \frac{\rho_p}{G_p} \right)^{\frac{1}{2}}$$

The correct choice of Rayleigh time scale plays a key role in the application of discrete element simulations. The same property related to the importance of the time scale is typical for all other methods based on an explicit time scale solution. The Rayleigh time step gives the amount of time a shock wave that passes through a grain particle.

Thus, when creating a discrete element model, it is necessary to specify the following micromechanical parameters:

- The Young modulus of the particle.
- Poisson's ratio of the particles.
- Density of the particles.
- Coefficient of friction between particles (this is not the internal coefficient of friction of the assembly).
- Coefficient of restitution between particles.
- Coefficient of rolling friction between particles.

Determining the value of the characteristics listed here by direct measurement is a rather difficult task according to Grima and Wyppych, 2010 [4]. For example, the modulus of elasticity, the Poisson's ratio, the coefficient of restitution and the coefficient of friction can be measured up to a certain size range, but there are also particle assemblies (e.g., dust, grits, soil) for which none of these particle characteristics can be measured.

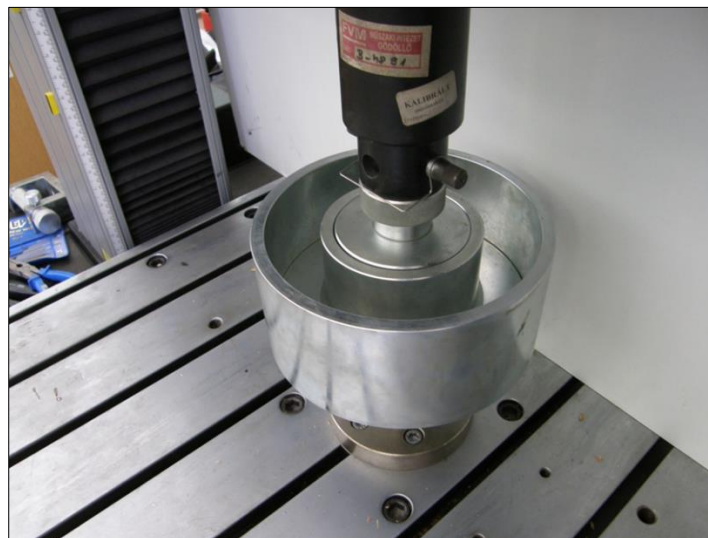


**Figure 2** Oedometric test

There is little data in the literature on the values of the above material parameters [5,6]. To perform the modelling tasks, I need a procedure to determine these micromechanical parameters. To do this, my team developed a specific procedure consisting of a combination of experimental studies and numerical simulations.

The initial assumption of the method is that no individual measurements are required to determine the mechanical parameters that are difficult or impossible to measure per eye. The assumption is that certain measurements performed on the assembly and their discrete element modelling allow the determination of the micromechanical characteristics of the assembly. If the values of the micromechanical parameters can be set during the simulation of the measurement so that the characteristics obtained during the simulation of the measurement fit well with the characteristics obtained during the measurement, then the micromechanical parameters thus determined give the mechanical properties of the particle assembly.

Measurements to determine the micromechanical characteristics of the particle set were previously performed with an Instron 5581 universal material tester. For the oedometric tests, a steel cylinder with a diameter of 100 and 200 mm and a height of 80 mm was manufactured, we used a piston for loading the particle assembly placed in the cylinder (Fig. 2).

For the discrete element simulation, we constructed the DEM model of the oedometer (Fig. 3). Hertz-Mindlin contact model was used to calculate the forces occurring during the interparticle contact.

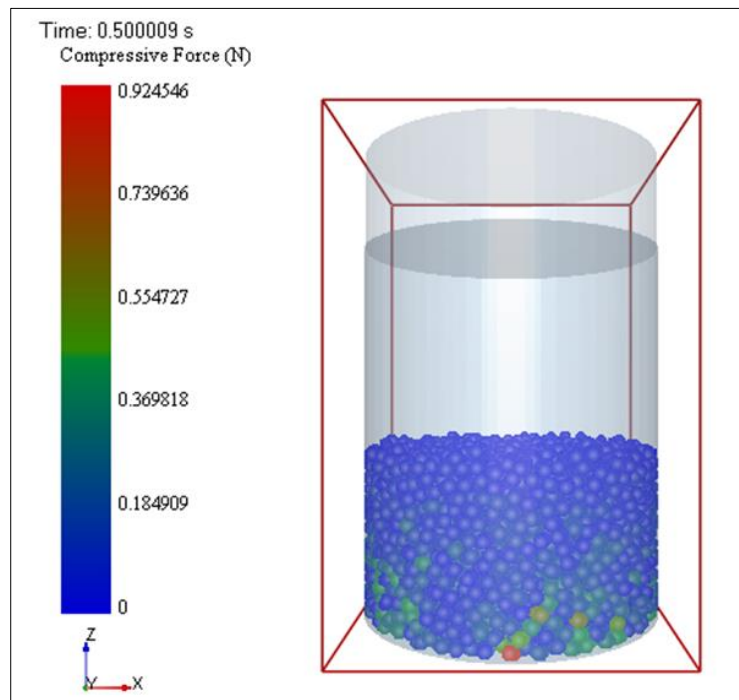


**Figure 3** DEM simulation of the oedometric test

The calibrated micromechanical parameters were the following:

- Shear modulus  $G = 3,58 \cdot 10^8$  Pa
- Poisson number:  $\nu = 0,4$
- Density of the particles  $\rho = 1430$  kgm<sup>-3</sup>.
- Coefficient of static friction  $\mu_s = 0.3$
- Coefficient of restitution  $c_r = 0.5$
- Coefficient of rolling friction  $\mu_r = 0.01$

In the discrete cell model, there is currently no way to completely fill a piece of equipment of this size and track the movement of the entire assembly. Fortunately, based on certain symmetry considerations, there is an opportunity to model a much smaller part.

A discrete element model was created for each particle first. Because DEM modelling uses shapes assembled from spheres to model the grains, as Tao et al. 2010 [7] describes that the particles are non-spherical, so I used three spheres that can be drawn inside a grain of wheat, for example. The geometry was a modified model of Keppler et. al. 2012 [8] (Fig. 4).

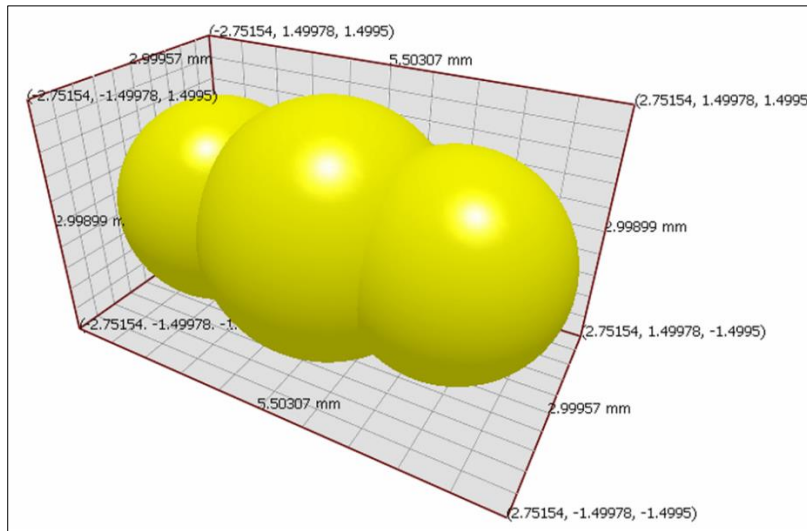


**Figure 4** DEM model of the particle

The kinematic boundary conditions in the case of the dryer are, on the one hand, the movement due to the gravitational field and, on the other hand, the interaction with the walls of the dryer.

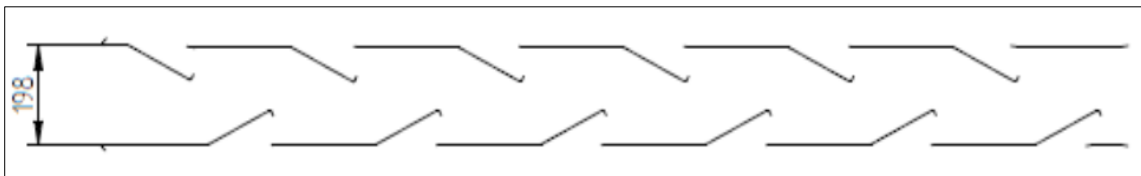


**Figure 5** Particle flow channel (the figure is rotated by 90 degree)

Instead of a complete dryer, the processes in the vicinity of only a few lamellas of one module were examined as shown in figure 5. A steel wall was provided on one side and a frictionless wall on the other side, the lower outlet and the upper inlet were connected by a periodic boundary, i.e., what fell out at the bottom was returned to the model at the top. With this, it became possible to work with a modelling-acceptable number of grains.

## 2. Results

During the simulations, we examined how the value of wall friction affects the velocity distribution of grain motion.

**Table 1** Simulation settings

Number	Wall friction	Particle-particle friction
1	0.1	0.1
3	0.1	0.5
5	0.1	0.9
7	0.2	0.1
9	0.2	0.5
11	0.2	0.9
13	0.3	0.1
15	0.3	0.5
17	0.3	0.9
19	0.4	0.1
21	0.4	0.5

23	0.4	0.9
25	0.5	0.1
27	0.5	0.5
29	0.5	0.9
31	0.6	0.1
33	0.6	0.5
35	0.6	0.9
37	0.7	0.1
39	0.7	0.5
41	0.7	0.9
43	0.8	0.1
45	0.8	0.5
47	0.8	0.9
49	0.9	0.1
51	0.9	0.5
53	0.9	0.9

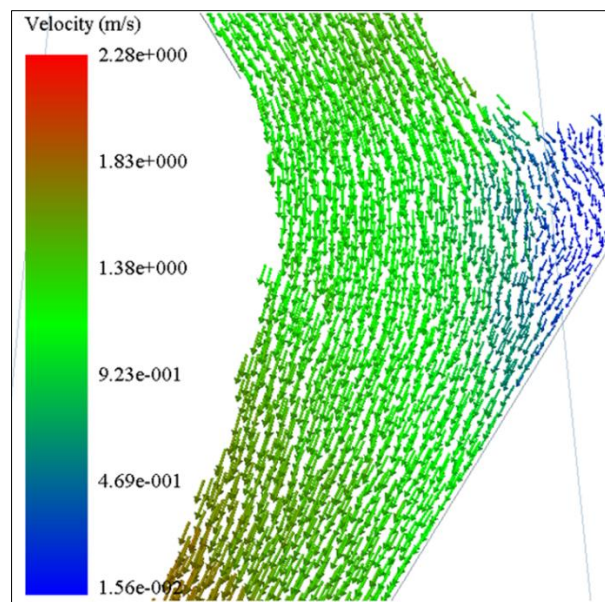


**Figure 6** Particle velocity distribution (case 27)

The example image above (Fig. 6) shows that the coefficient of static friction has a significant effect on the particle velocity distribution. If we take a closer look at the flow velocity vector field, we can see that there are slow zones around the baffles and the sidewall. In the immediate vicinity of the intersection of the baffles and the wall, the particles move back and forth at a very low speed, with no clear downward flow in that part.

Further increasing the particle-particle and particle-wall coefficient of friction we get the following figure (Fig. 7).

Examining figure 7, we can see that the maximum velocity did not change compared to the case of moderate friction values, but the material stopped at several places along the wall, and a “tear” can also be seen in the assembly. At this point, the flow rate is almost two orders of magnitude lower, and the movement has almost completely stopped. Examining the velocity distribution, we can see that a significant part of the flowing material has slowed down.

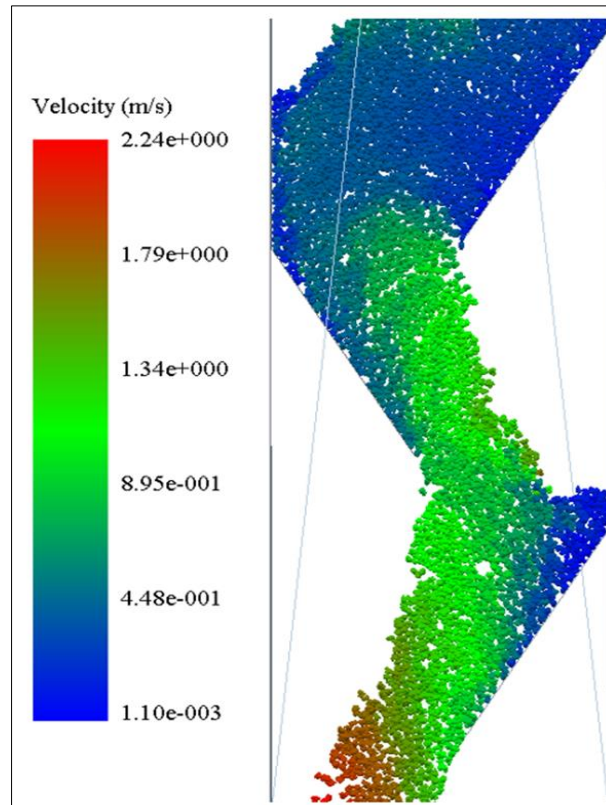


**Figure 7** Particle velocity distribution in case of large friction values

### 3. Conclusion

The material flow processes in the dryer are significantly affected by the coefficient of static friction of the material to be dried. We could see that as the internal friction of the material increased, the flow mass flow gradually decreased, and then dormant, jammed zones appeared in the vicinity of the baffles and vertical walls, which also caused a quality change in the flow field. During drying, as the contamination of the particulate material increases, the particle-wall and particle-particle friction also increases. Because of this, a main flow channel is formed in the module, as well as a zone where there is no significant material movement.

Differences in flow rates of this nature have a significant effect on the unevenness of the moisture content of the dried material, since the material which remains in the drying chamber for an unnecessarily long time is over-dried and the under-drying is a problem for the material remaining in the dryer for too short a time.

### Compliance with ethical standards

#### *Acknowledgments*

The author appreciates the assistance of his colleagues during the research project.

#### *Disclosure of conflict of interest*

The author has declared that there is no existence of competing interests.

### References

- [1] J Mellmann, T Teodorov. Solids transport in mixed-flow dryers: Powder Technology. 2011; 205: 117–125.
- [2] J Mellmann, KL Iroba, T Metzger, E Tsotsas, C Mészáros, I Farkas. Moisture content and residence time distributions in mixed-flow grain dryers, Biosystems Engineering. 2011; 109(4): 297–307.

- [3] Peter A Cundall, Otto DL Strack. A discrete numerical model for granular assemblies, *Geotechnique*. 1979; 3: 47-65.
- [4] AP Grima, PW Wypych. Development and validation of calibration methods for discrete element modelling, *Granular Matter*. 2010.
- [5] CJ Coetzee, Review: Calibration of the discrete element method, *Powder Technology*. 2017; 310: 104-142.
- [6] Corné Coetzee, Calibration of the discrete element method: Strategies for spherical and non-spherical particles, *Powder Technology*. 2020; 364: 851-878.
- [7] He Tao, Baosheng Jin, Wenqi Zhong, Xiaofang Wang, Bing Ren, Yong Zhang, Rui Xiao, Discrete element method modeling of non-spherical granular flow in rectangular hopper, *Chemical Engineering and Processing*. 2010; 49: 151–158.
- [8] Istvan Keppler, Laszlo Kocsis, Istvan Oldal, Istvan Farkas, Attila Csatar: Grain velocity distribution in a mixed flow dryer, *Advanced Powder Technology*. 2012; 23(6): 824-832.